Appl. Phys. A 66, S337–S340 (1998)

Applied Physics A
Materials
Science & Processing

Charge distribution on photorefractive crystals observed with an atomic force microscope

E. Soergel[1], **W. Krieger**[1], **V.I. Vlad**[2]

[1] Max-Planck-Institut für Quantenoptik, Hans-Kopfermann-Strasse 1, D-85748 Garching, Germany
[2] Institute for Atomic Physics, Department of Lasers, R-79600 Bucharest, Romania

Received: 25 July 1997/Accepted: 1 October 1997

Abstract. Electrostatic force detection with an atomic force microscope (AFM) is applied to the study of light-induced charge gratings on photorefractive materials. These gratings are generated by two crossed laser beams at a wavelength of 514 nm in $Bi_{12}SiO_{20}$ and $BaTiO_3$ crystals. In contrast to conventional optical investigations of photorefractivity, where volume gratings of the refractive index are indirectly observed, the AFM allows a direct study of the charge gratings at the surface. Charge images of the two crystal materials are compared. The saturation of the charge gratings at increasing laser fluence is measured for both materials. From the observation of the phase shift between the light-intensity grating and the charge grating, the polarity of the charge carriers in $Bi_{12}SiO_{20}$ is determined.

The atomic force microscope (AFM) is by the far the most versatile instrument of the growing family of scanning probe microscopes. This is due to the multitude of different forces that can be studied with this instrument. In this paper, we present an application of the AFM to the measurement of electrostatic forces for the detection of light-induced charge distributions on photorefractive crystals.

Photorefractive materials are of growing interest because of their applications in such fields as high-density optical data storage, real-time holography and optical phase conjugation, to name but a few. The photorefractive effect occurs in crystals that are both photoconducting and electro-optic [1]. In these materials, a spatially modulated light-intensity distribution, e.g. a light grating generated by the interference of two laser beams, is used to excite charge carriers. These carriers are redistributed by drift and diffusion until they are trapped to form a space–charge distribution. The accompanying electrostatic fields lead to a refractive-index pattern via the electro-optic effect. In the case of a grating, it is easily seen how this can be "read" by Bragg diffraction.

In such an experiment, as in most of the conventional methods for investigating photorefractivity, the properties of the bulk of the material are studied. Increasingly, however, photorefractive materials are used as thin films, waveguides and optical fibers [2], and in these instances surface effects begin to be important. A surface-specific study of photorefractivity therefore becomes desirable. Electrostatic force microscopy, which allows the study of light-induced charge distributions at the surface of photorefractive materials, is ideal for this purpose. A sensitive method for charge detection on insulating surfaces was introduced by Terris et al. [3], and it was later applied by Schönenberger to image single electrons [4].

A first demonstration of light-induced charge gratings on $BaTiO_3$ crystals was recently reported [5]. Here we present a detailed study of such gratings on $Bi_{12}SiO_{20}$ (BSO) and on $BaTiO_3$. A surface-specific microstructure in the charge images is revealed, and a saturation of the gratings at increasing light fluence was observed. In addition, we report simultaneous measurements of the light-intensity grating and the charge grating on both materials. This has allowed us to determine the sign of the charge carriers responsible for the grating formation, and gives information on internal crystal fields.

1 Experimental method

The experimental setup is shown in Fig. 1. The force sensor of our home-built AFM used the beam-deflection technique. In order to prevent the laser radiation of the force sensor from reaching the photorefractive sample and erasing the stored charges, the back of the silicon cantilever was covered with an aluminum layer of 60 nm in thickness. The AFM was operated in non-contact mode. The cantilever was excited at its resonance frequency ($\omega_1 \approx 60$ kHz) by a piezo, and the oscillation amplitude was kept constant. Typical tip–sample distances used were 10 nm.

For charge detection, a voltage $V_0 \cos \omega_2 t$ ($V_0 = 2.5$ V, $\omega_2 = 2$ kHz) was applied to the tip. The electrostatic force between the periodic charge at the tip and the surface charge to be measured was detected with lock-in amplifier no. 2 at frequency ω_2. The phase of this lock-in amplifier was set to give a positive output signal (bright image area) when the AFM tip was above a negative surface charge and a negative output signal (dark area) for a positive charge. This adjustment was controlled using small surface charges deposited by voltage pulses of ± 10 V and 20 ms duration applied to the tip. Im-

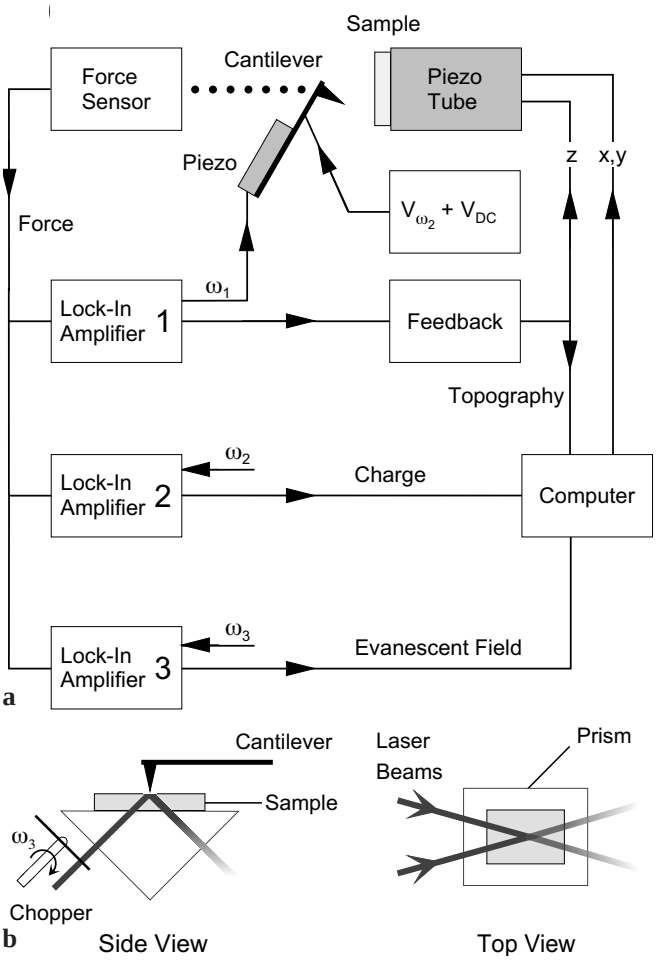

Fig. 1a,b. Schematic drawing of the experimental setup: **a** measurement of the electrostatic force with the AFM; **b** optical setup for the generation of charge gratings in a photorefractive sample

ages of the topography and the charge signal were acquired simultaneously.

The charge gratings in the photorefractive crystals were generated by two argon-ion laser beams at wavelength $\lambda = 514\,\text{nm}$ in a total-internal-reflection geometry, as shown in Fig. 1b. The grating period was able to be varied between $1.5\,\mu\text{m}$ and $10\,\mu\text{m}$, and the polarization direction was perpendicular to the plane of incidence. The detection of the evanescent field of the writing beams is based on the generation of a surface photovoltage in the Si tip of the AFM [5]. The writing beams were chopped at frequency $\omega_3 = 800\,\text{Hz}$, and the signal was measured with lock-in amplifier no. 3. For simultaneously recording the evanescent field of the writing beams and the charge distribution generated in the crystal, we scanned the complete cantilever-force-sensor assembly with the help of piezo stacks.

The AFM was housed in a light-tight box which was flooded with dry nitrogen. This was found necessary after measurements of the decay time of surface charges on BSO crystals had shown a strong dependence on the relative humidity. The photorefractive samples studied were two $Bi_{12}SiO_{20}$ crystals (no. 1 [6] and no. 2 [7]) and one $BaTiO_3$ crystal [8]. They were brought into optical contact with BK7 prisms as shown in the Fig. 1b.

2 Results

In Fig. 2 we present images of the crystal topography (a) and of the electrostatic force (b), simultaneously recorded on BSO crystal no. 1. The crystal had been illuminated for 10 s with two laser beams of $135\,\text{mW/cm}^2$. The topography shows a large number of scratches, as is typical for polished surfaces. On the electrostatic force image in Fig. 2b, a vertical grating with the expected period of $2.5\,\mu\text{m}$ is observed. The amplitude of the charge grating corresponds to a force of $\approx 15\,\text{pN}$. Superimposed on the grating are thinner lines carrying negative charges. These were already present before the generation of the charge grating. Most of the charged lines are correlated with scratches in the topography. Examples are

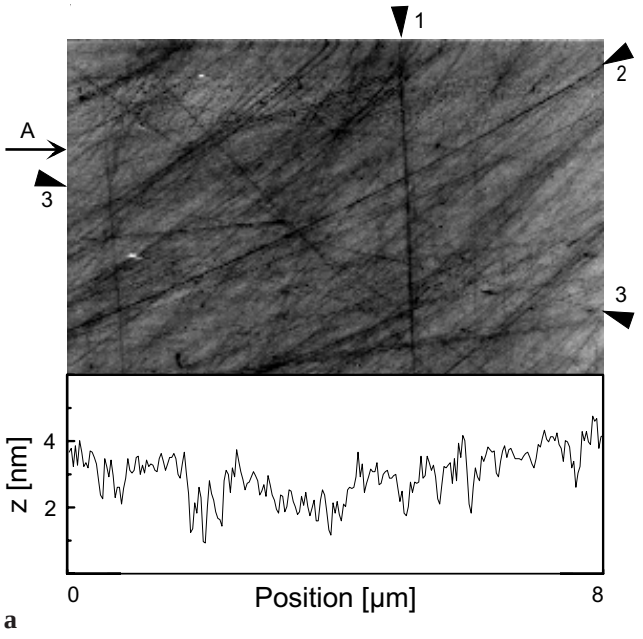

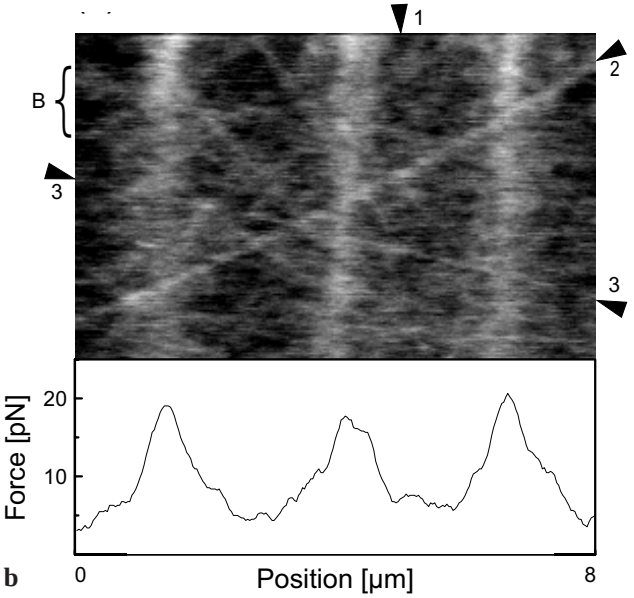

Fig. 2a,b. Topography (**a**) and simultaneously recorded charge signal (**b**) on BSO crystal no. 1 (image size $8 \times 5\,\mu\text{m}^2$, acquisition time 5.5 min). In **a**, the lower part shows a line scan at position A; in **b**, it shows an average over 30 lines at position B. Three scratches are indicated by numbered triangles

scratches numbered 2 and 3 in the figure. No charges are accumulated, however, on the scratch numbered 1.

Figure 3 shows corresponding images of the topography (a) and the electrostatic force (b) for the $BaTiO_3$ crystal. The charge grating was generated using $135\,mW/cm^2$ and a writing time of 120 s. The amplitude of the charge grating corresponds to a force of ≈ 10 pN. On the topography, polishing traces are detectable but less conspicuous than on the BSO crystal. The microstructure of the charge signal is less pronounced. There is an indication also of positively charged lines. In the upper-right corner, a large positively charged area is observed, and this is also visible in the averaged scan.

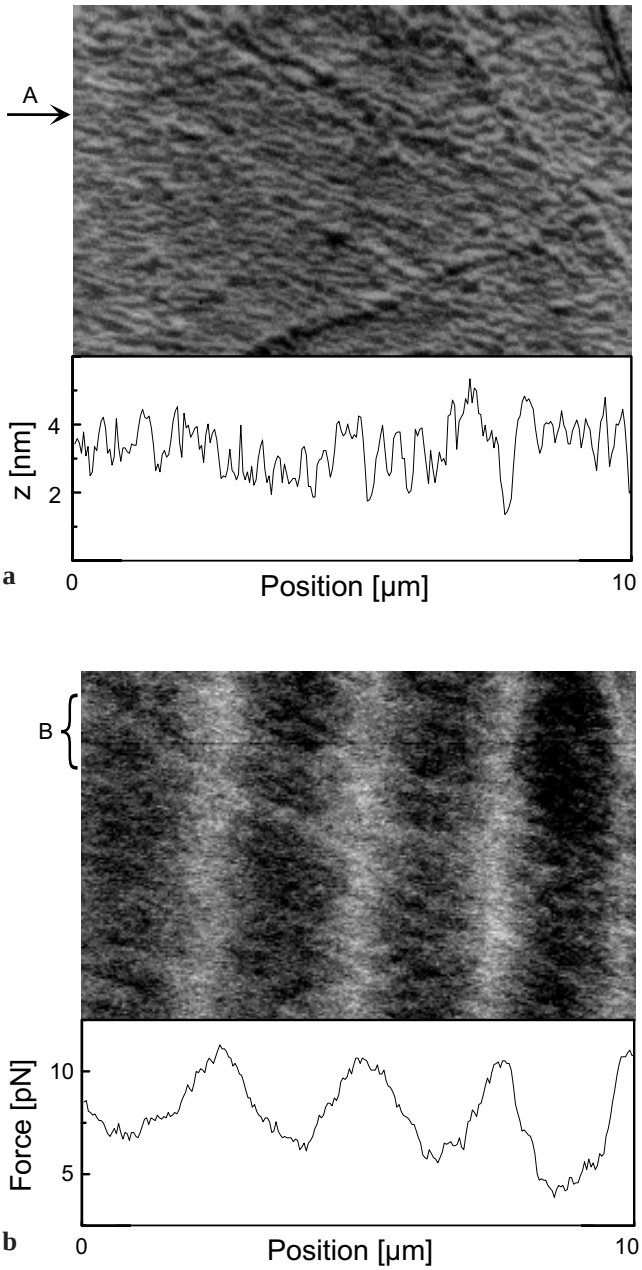

Fig. 3a,b. Topography (**a**) and simultaneously recorded charge signal (**b**) on the $BaTiO_3$ crystal (image size $10 \times 6\,\mu m^2$, acquisition time 13 min). In **a**, the lower part shows a line scan at position A; in **b**, it shows an average over 30 lines at position B

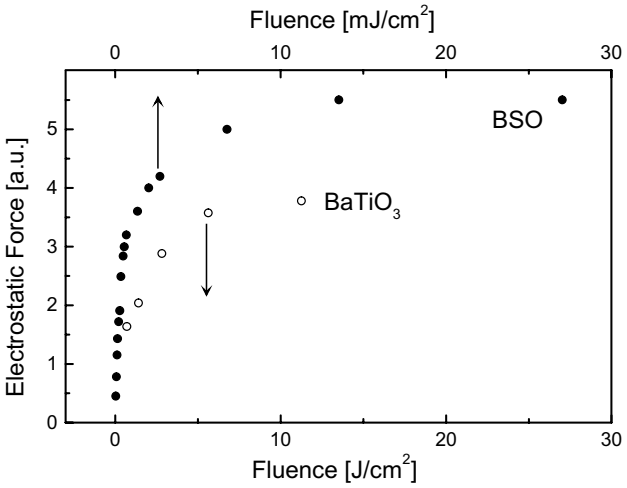

Fig. 4. Saturation of the grating amplitude in BSO crystal no. 2 (*solid circles*) and in the $BaTiO_3$ crystal (*open circles*)

The photorefractive effect is known to saturate at increasing writing fluences. We investigated the saturation process by plotting the amplitude of the charge gratings as a function of the writing fluence (Fig. 4). The experiments were performed at constant laser intensity ($1.35\,mW/cm^2$ per beam for BSO, and $70\,mW/cm^2$ for $BaTiO_3$) and with variable writing times. It is immediately seen that the laser fluence necessary to set up a saturated grating in the two crystals differs by approximately a factor of 1000 ($\approx 10\,mJ/cm^2$ for BSO vs. $\approx 10\,J/cm^2$ for $BaTiO_3$). In the BSO crystal, the grating amplitude is a linear function of the fluence only below $0.5\,mJ/cm^2$.

Finally we consider the polarity of the stored charge grating. We know that the bright grating lines in the image correspond to negatively charged areas. This information becomes relevant if we succeed in correlating the light grating with the induced charge grating. This is possible by a simultaneous measurement of the evanescent field and the charge grating. The results of these measurements are displayed in Fig. 5a for BSO crystal no. 2 and in Fig. 5b for the $BaTiO_3$ crystal. An evaluation of the data shows that for BSO the maxima of the charge grating are shifted with respect to the minima of the evanescent field grating by only $6 \pm 3°$ – in other words, negative charges accumulate roughly at the dark grating lines. In $BaTiO_3$, however, we observe a much larger shift of $59 \pm 4°$. A similar measurement on $BaTiO_3$ [9] cannot be compared with our results since no information on the charge polarity is given.

3 Discussion

Electrostatic force imaging provides interesting new possibilities for the study of photorefractivity. For the first time, direct images of the light-induced charge distributions can be recorded with a spatial resolution of a few tens of nanometers. Higher resolution can be obtained by force–gradient imaging, since the gradient shows a steeper decrease along the surface normal.

The charge images reveal a microstructure not observed before. As seen in many images, some of the features are correlated with topographical details, such as charges accumu-

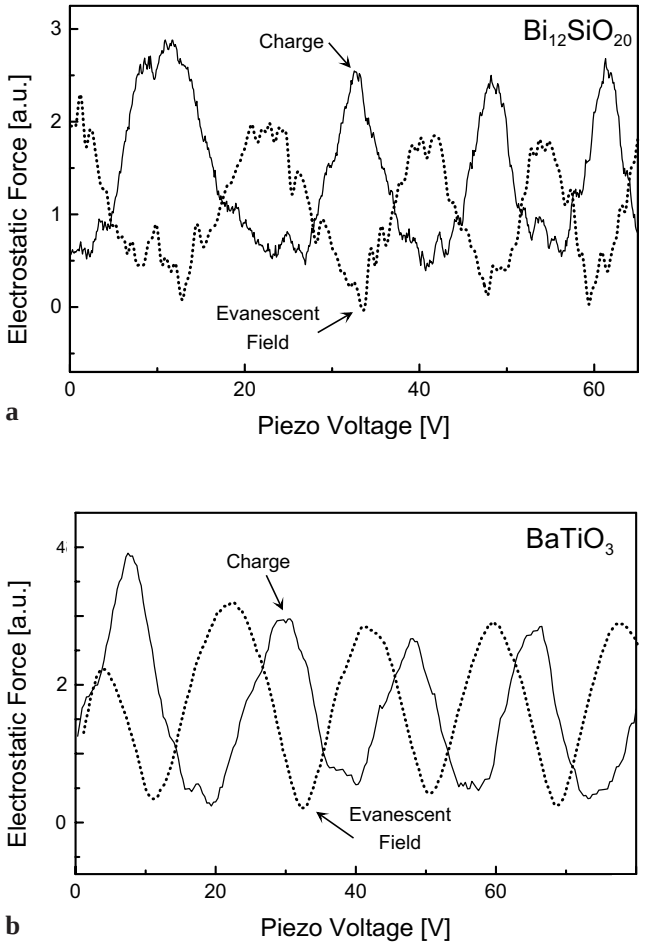

Fig. 5a,b. Simultaneous measurement of the charge signal and the signal of the evanescent field on a BSO crystal no. 2 (**a**) and (**b**) on the $BaTiO_3$ crystal

lated along scratches or charged spots at adsorbed nm-sized particles. This stresses the importance of careful surface preparation. However, we also observed charged areas not connected with the topography. These may be due to traps located at larger crystal defects. Finally, at higher spatial resolution, we expect to see a microstructure caused by the statistical distribution of single traps in the crystal.

The electrostatic force amplitudes of the gratings in Figs. 2 and 3 for BSO and $BaTiO_3$, respectively, have comparable values in the pN range. From the force amplitudes, the charge densities in the grating can be calculated if the tip radius, and therefore the tip–sample capacitance are known [10]. Since both images were obtained with the same tip, however, we are able to conclude that also the charge densities in the grating lines for both materials have comparable values. As the laser fluence for both cases was in the saturating regime, we can roughly identify these charge densities with the density of empty traps in both materials. Indeed, these densities, as given in the literature, also have comparable values (1×10^{-16} cm^{-3} for BSO and as 0.5×10^{-16} cm^{-3} for $BaTiO_3$ [11]).

We want to point out again, however, that we have compared bulk values of the crystal parameters, as obtained by conventional methods, with surface values as obtained with the AFM, where the AFM has collected data from a surface layer with a thickness given by the range of the electrostatic force. From the distance dependence of the electrostatic force over small charged surface areas, we estimate that this surface layer is roughly 10 nm thick. The properties of this layer may differ considerably from the bulk of the sample by adsorbates, diffused particles or the effects of surface preparation.

Saturation of the photorefractive effect cannot only be observed as a nonlinear change of the amplitude of the charge grating as shown in Fig. 4. Electrostatic force imaging allows us to observe this process directly as a change of the line shape of the charge grating. The sinusoidal shape of the linear regime is expected to be more and more deformed at higher fluences. This behavior is particularly well observed in BSO [10]. An example of such a saturated line shape is seen in Fig. 2b.

Finally, we discuss the phase difference between the light and the charge grating measured in the two types of crystal. Assuming diffusion-dominated charge transport (i.e., no internal or external fields present), it is expected that the mobile charge carriers accumulate at the dark grating lines. For BSO crystal no. 2, where negative charges are observed at the dark lines, it follows immediately that the mobile charge carriers are predominantly electrons. This was also found for BSO in former experiments [12].

The large shift of $59 \pm 4°$ observed between the dark lines and the maxima of the charge signal in the $BaTiO_3$ crystal can only be explained by internal electric fields causing a drift of the charge carriers. In $BaTiO_3$ these fields can be of piezoelectric or ferroelectric origin. Piezoelectric fields are excluded in our geometry because of the relative orientation of the *c*-axis and the grating *k*-vector. Further experiments are necessary to verify whether or not the ferroelectric fields can cause the observed phase shift.

Acknowledgements. We gratefully acknowledge enlightening discussions with K. Buse.

References

1. See, for example, the recent review articles by K. Buse, Appl. Phys. B **64**, 273 (1997) and B **64**, 391 (1997)
2. D.D. Nolte (Ed.): *Photorefractive Effects and Materials* (Kluwer, Boston 1995)
3. B.D. Terris, J.E. Stern, D. Rugar, H.J. Mamin: Phys. Rev. Lett. **63**, 2669 (1989)
4. C. Schönenberger: Phys. Rev. B **45**, 3861 (1992)
5. M. Hipp, J. Mertz, J. Mlynek, O. Marti: In *Photons and Local Probes*, ed. by O. Marti, R. Möller (Kluwer, Dordrecht 1995)
6. $Bi_{12}SiO_{20}$ crystal no. 1 from Alkor Technologies, St. Petersburg, Russia. Size $2 \times 5 \times 6$mm^3, orientation (110), undoped
7. $Bi_{12}SiO_{20}$ crystal no. 2 from the Institute for Atomic Physics, Bucharest, Romania. Size $2 \times 7 \times 8$mm^3, transverse orientation, undoped
8. $BaTiO_3$ crystal from CASIX Inc., Fuzhou, Fujian, PR China. Size $1 \times 5 \times 6$mm^3, orientation (110), undoped
9. M. Hipp: *Konstanzer Dissertationen* (Hartung Gorre Verlag, Konstanz 1994)
10. E. Soergel, W. Krieger, V.I. Vlad: to be published
11. J.W. Yu et al.: In *Photorefractive Materials and their Applications II*, ed. by P. Günther, J.-P. Huignard, Topics Appl. Phys., Vol. 62 (Springer, Berlin 1989); M.B. Klein: In *Photorefractive Materials and Their Applications I*, ed. by P. Günther, J.-P. Huignard, Topics Appl. Phys., Vol. 61 (Springer, Berlin 1988)
12. G.C. Valley, M.B. Klein: Opt. Eng. **22**, 21 (1983); S.I. Stephanov, M.P. Petrov: In *Photorefractive Materials and their Applications I*, ed. by P. Günther, J.-P. Huignard, Topics Appl. Phys., Vol. 62 (Springer, Berlin 1988); L. Arizmendi, J.M. Cabrera, F. Agnello: Int. J. Optoelectron. **7**, 149 (1992)